

## **W-BAND MICROSTRIP-TO-WAVEGUIDE TRANSITION USING VIA FENCES**

**R. Shireen, S. Shi, and D. W. Prather**

Department of Electrical and Computer Engineering  
University of Delaware  
Newark, DE-19716, USA

**Abstract**—The paper presents integrated probe for direct coupling to the WR-10 waveguide with the use of metal filled vias on both sides of the microstrip line. Design and optimization of this novel microstrip-to-waveguide transition has been performed using 3-D finite element method based software HFSS (High Frequency Structure Simulator). A back-to-back transition has been fabricated and measured between 75–110 GHz. The measured return loss is higher than 10 dB and the insertion loss for a single microstrip-to-waveguide transition is about 1.15 dB.

### **1. INTRODUCTION**

Monolithic and hybrid integrated circuits are widely used for wireless communications, radar sensors and imaging receivers. Despite numerous applications of microstrip line in the field of millimeter-wave integrated circuits, waveguides are still necessary for low loss, robustness and compatibility with some type of antennas. The interface between the MMIC (Monolithic Microwave/Millimeter-wave Integrated Circuit) and the waveguide plays an important role in determining the loss, noise performance, bandwidth, and the size of a system.

Several microstrip-to-waveguide transitions have been published in the past, such as transitions using monopole Yagi-Uda antenna [1], antipodal finline [2] and quasi-Yagi antenna [3]. These types of transitions are designed along the propagation direction of the waveguide and can only be applicable for W-band (75–110 GHz) operations if low dielectric constant materials are used to prevent

higher order mode. An end-wall transition based on slot-coupled antenna is presented for high dielectric constant material alumina ( $\epsilon_r = 9.8$ ) in [4]. But the transition gives rise to the difficulty of placing the antenna substrate in the stepped waveguide. Another type of transition commonly used for packaging launches a longitudinal  $E$ -field probe transverse to the propagation direction of the waveguide. But the width of the probe substrate has to be less than  $\lambda_d/2$  to prevent excitation of the dielectric filled quasi-rectangular waveguide mode propagation along the microstrip line, where  $\lambda_d$  is the wavelength in the dielectric medium. According to [5], the width of alumina substrate has to be 500  $\mu\text{m}$  for W-band operation. But most of the active/passive chips are much wider and range from 1 to 1.5 mm wide. Figure 1 shows the change in transition parameters as the substrate width  $W_s$  is changed from 0.5 mm to 1.5 mm. The presence of dielectric waveguide mode drastically changes the transmission characteristics. A solution to this problem is proposed in [6] consisted of a disk shaped patch antenna at the end of microstrip line. The shape of the substrate is modified to fit into the aperture cut in the waveguide. But the transition doesn't cover the entire W-band. Moreover, the presence of metallic parts near the patch antenna makes the design susceptible to parasitic mode coupling.

For packaging, the probe is frequently fabricated on a separate substrate apart from the MMICs and ribbon bonding is used to connect them. If the bond length is not made short enough, the discontinuity introduced by the bonding wire can significantly degrade the performance of the millimeter-wave circuits. In [7], the probe

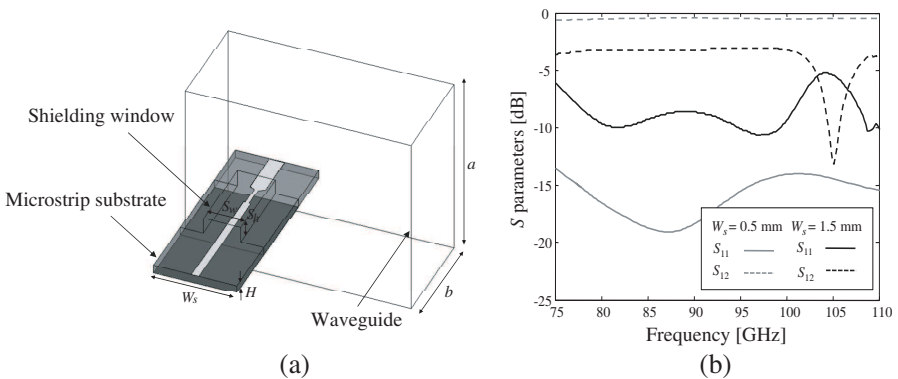


**Figure 1.** (a) Configuration of the conventional microstrip-to-waveguide transition without via fences and (b) the effect of substrate width on the transition performance.

is integrated monolithically with the amplifier to provide interface between the MMIC and the waveguide. To suppress the unwanted waveguide mode, a large number of vias connecting the top and bottom grounds of the grounded coplanar waveguide are formed in the substrate. In this paper, the method used to improve the isolation between the two microstrips using continuous via fence, is adopted [8]. Electroplated vias are placed on both sides of the microstrip line to synthesize electrical walls and thus make the effective width of the substrate narrower than the actual width. The idea overcomes the restriction on the substrate with and can be implemented to directly integrate the probe with other active/passive circuit elements for waveguide-based packaging.

## 2. DESIGN

The substrate material used for the design is 99.6% alumina, which has a dielectric loss tangent of 0.002 at W-band. The required vias can be drilled in the alumina substrate using well known laser ablation technique. Although etching vias in silicon or gallium arsenide substrate is not very difficult, alumina is easier to handle when it is 100  $\mu\text{m}$  thick. The dielectric constant  $\epsilon_r$  of 9.8 makes it compatible with other commonly used MMIC chip substrates (indium phosphide, gallium arsenide). The width  $W_s$  is chosen to be 1.5 mm, which represents width of most of the MMIC chips used at millimeter-wave frequencies.

The proposed transition is illustrated in Figure 2. The radiating element of the transition is a rectangular probe pad that extends

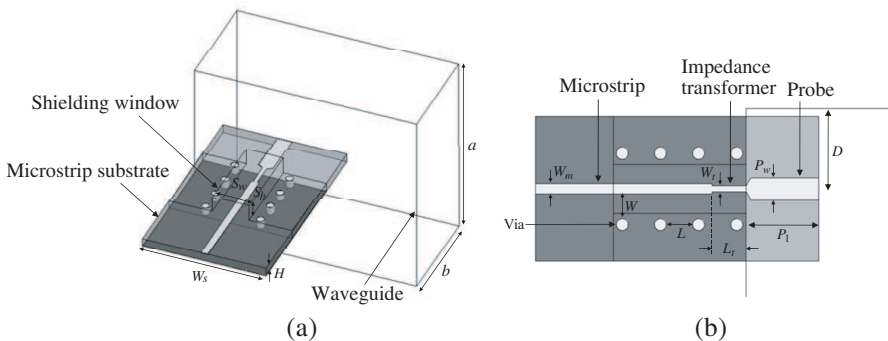


**Figure 2.** Configuration of the new microstrip-to-waveguide transition (a) 3-D view and (b) top view.

roughly halfway into the waveguide from an inverse T-shaped aperture cut at the center of the broad wall and is aligned with the direction of propagation. The shielding window of the microstrip line needs to be small enough to minimize the electric field perturbation in the waveguide. The width  $S_w$  and height  $S_h$  of the shielding window are  $450\ \mu\text{m}$  and  $200\ \mu\text{m}$ , respectively. The designed probe pad size is  $P_l \times P_w = 565\ \mu\text{m} \times 185\ \mu\text{m}$  and the distance  $D$  between the center of the probe and the backshort is  $855\ \mu\text{m}$ , which is about quarter-wavelength to achieve maximum electric field near the probe. The ground plane at the back side of the substrate is removed beneath the probe. A quarter-wavelength impedance transformer of width  $W_t = 48\ \mu\text{m}$  and length  $L_t = 275\ \mu\text{m}$  is designed around  $95\ \text{GHz}$  to match the probe impedance with the microstrip line.

Throughout this paper, the default value for the strip width  $W_m$  is  $90\ \mu\text{m}$  to result in a  $50\ \Omega$  characteristic impedance for an alumina substrate of thickness  $H = 100\ \mu\text{m}$ . For the design, the diameter of the via hole is  $75\ \mu\text{m}$ . The transmission characteristics of this transition is mainly controlled by the spacing between the via hole and microstrip,  $W$  and the distance between the adjacent via holes,  $L$ . To analyze the influence of vias, the transmission coefficients of the microstrip-to-waveguide transition are calculated. The simulation is carried out over  $75\text{--}110\ \text{GHz}$  for the following three cases  $W/H = 2, 2.5$  and  $3$  while keeping the value of  $L/H$  fixed at  $2.5$ . In case of  $W/H = 2$ , when the vias are brought closer to the microstrip line significant fields leak out from the via fences as shown in Figure 3(b). The fields between the via fences and the metallic wall of the housing cause the resonance to occur at  $102.5\ \text{GHz}$ . When  $W/H = 2.5$  resonance free operation can be achieved within the frequency band of interest. The plot in Figure 3(c) shows that the electric fields are confined near the microstrip line. Finally, for the case of  $W/H = 3$ , the spacing between the via fences is more than  $\lambda_d/2$ , the structure supports higher order mode to propagate between the metal fences as shown in Figure 3(d). The dips in transmission can be observed at  $101$  and  $109\ \text{GHz}$  in Figure 3(a).

Next, the transmission coefficients are calculated by varying both  $W/H$  and  $L/H$  to find out the acceptable operating frequency range. The transition performance is considered satisfactory as long as the magnitude of transmission coefficient  $S_{12}$  is less  $1.5\ \text{dB}$ . In Figure 4, the vertical axis denotes the highest operating frequency at which  $S_{12}$  is more than  $1.5\ \text{dB}$ . The drop in transmission is occurred due to i) the presence of dielectric filled waveguide mode when  $W/H > \lambda_d/2$  and ii) the leakage of energy from microstrip line mode when the vias are close to the microstrip. The shaded area represents the operating

frequency range of the standard WR-10 waveguide. When  $W/H = 3$ , the resonance condition occurs within the frequency band of interest for all the values of  $L/H$ . The graph indicates that closely spaced via holes confine the electromagnetic field while the widely spaced via holes allow leakage of power. As a result, when  $L/H > 2$  the electromagnetic fields that exist beyond the via fence give rise to standing wave pattern between the via fence and the waveguide wall at certain frequencies.

The sensitivity analysis of the transition is performed to find out the effect of assembly tolerances. Figures 5 and 6 show the change in  $S_{12}$  as a result of translation of the substrate with respect to the waveguide along  $x$  and  $y$  directions, respectively. The shifts do not seem to affect the performance significantly over most of the operating

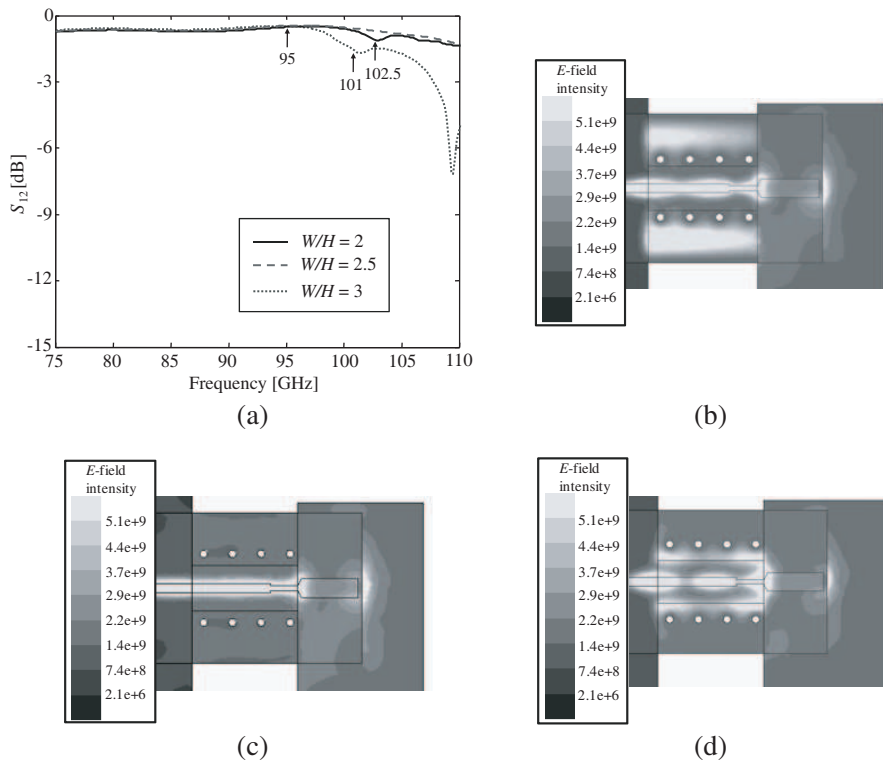


**Figure 3.** (a) Simulated transmission coefficients of the transition for different values of  $W/H$ , electric field intensity distribution across the microstrip line substrate (b) at 102.5 GHz when  $W/H = 2$ , (c) at 95 GHz when  $W/H = 2.5$ , and (d) at 101 GHz when  $W/H = 3$ .

band. Tolerance analysis is also carried out based on the information provided by the laser-drilling manufacturer. The tolerance for the diameter and position of the laser drilled vias are  $\pm 5 \mu\text{m}$  and  $\pm 2 \mu\text{m}$ , respectively. Within W-band, the maximum variation in insertion loss for the via diameter tolerance is 0.03 dB. However, the insertion loss is not affected by the positional tolerance of the vias.

### 3. FABRICATION

To experimentally evaluate the performance, transition consisting of input and output microstrip lines with a 1 cm long waveguide section in between them is fabricated. Figure 7 explains the process flow followed to fabricate the vias and the microstrip line. Vias with diameter of  $75 \mu\text{m}$  are drilled using laser ablation for the spacing of  $W/H = 2.5$  and  $L/H \approx 2.5$ . The separation between the vias is chosen  $L/H \approx 2.5$  for the design to comply with the standard fabrication process. The Seed layers consisting of TiW/Au/TiW-100/180/60 nm are sputtered deposited on the top surface of the wafer. During this step, sidewalls of the tapered via holes are also partially covered with metallization layers as the laser drilled via holes have uniform taper to the sidewalls. Next,  $5 \mu\text{m}$  thick SU-8 is spray coated on the sample and the signal electrode pattern along with the circular-shaped openings for vias are transferred to the photoresist. After electroplating step, the remaining photoresist is removed and seed layers are sputtered at the back side. The photoresist is again spray coated on both sides of the wafer and the ground plane is patterned at the backside as well as vias are opened on the top side in the second photolithography step. The vias are

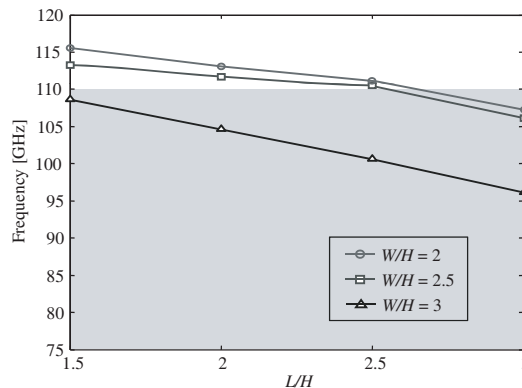


**Figure 4.** Graph of highest operating frequency as a function of  $W/H$  and  $L/H$ .

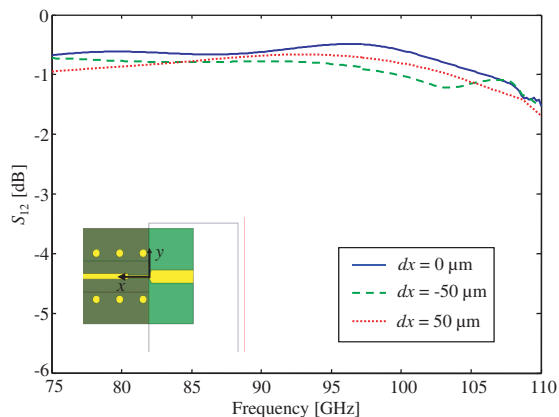


**Figure 5.** Sensitivity of  $S_{12}$  to a translation along  $x$  direction.

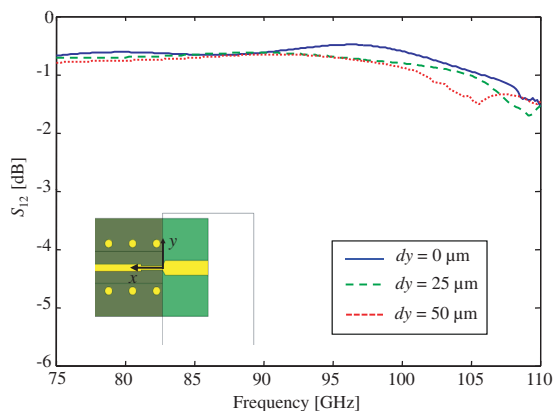


**Figure 6.** Sensitivity of  $S_{12}$  to a translation along  $y$  direction.

electroplated for the second time just to make sure the entire side walls are plated with gold. After removal of the photoresist, the sample is diced to a size of  $2.9 \text{ mm} \times 1.5 \text{ mm}$ .

The waveguide is made out of four aluminum blocks as shown in Figure 8. The bottom half of the waveguide has  $1500 \mu\text{m}$  wide and  $150 \mu\text{m}$  deep grooves, which serve as the cradle for the fabricated probes. Also, two grooves are machined in the top half of the waveguide block function as the shields for the microstrip lines. Both the width and the depth of each waveguide half machined into the metal block are  $1.27 \text{ mm}$ . The other two metal blocks are screwed from the sides to complete the housing.

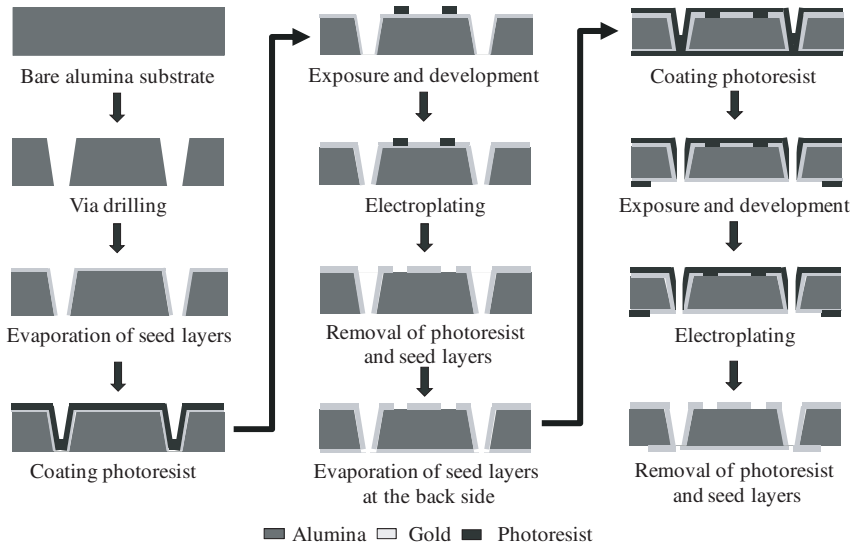


**Figure 7.** Fabrication steps.

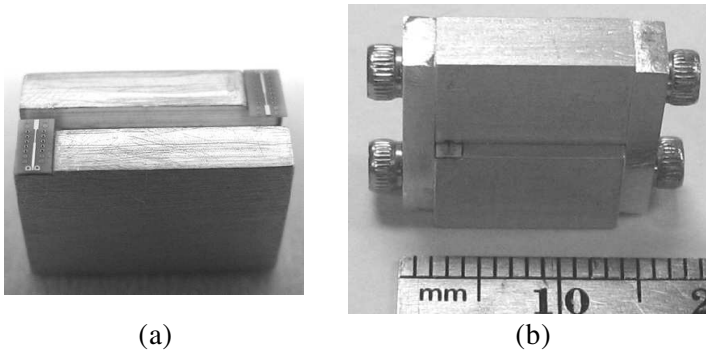


**Figure 8.** Photograph of the (a) bottom half of the waveguide with microstrip substrates placed on the cradle and (b) fully integrated microstrip-to-waveguide assembly.

#### 4. MEASUREMENT

The fabricated transition is measured in a back-to-back configuration using an HP8510C vector network analyzer. In W-band, the measured insertion loss is about 3.2 dB, which includes losses in the 1 cm long waveguide, two 2 mm long microstrip lines and two microstrip-to-waveguide transitions. The standard WR-10 waveguide ( $a = 2.5$  mm,

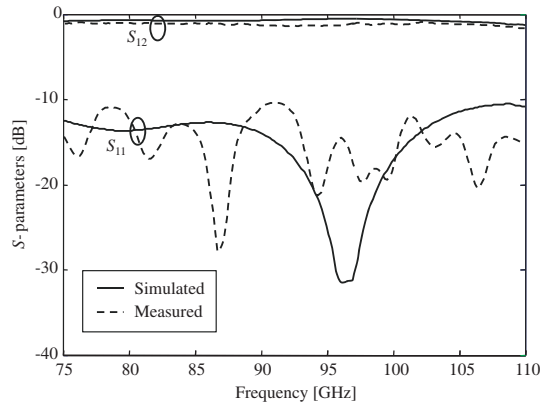


**Figure 9.** Simulated and measured results of a single microstrip-to-waveguide transition.

$b = 1.27$  mm) has loss of 0.04 dB/cm and the measured microstrip line loss is about 0.25 dB/mm in this frequency band. The extracted insertion loss for each transition is about 1.15 dB as shown in Figure 9.

## 5. CONCLUSION

The  $E$ -plane probe with via fence is well suited for simple and compact integration of the planar circuits with rectangular waveguide. To avoid dielectric filled waveguide mode within the W-band, via fences should be kept at least 2.5 times the substrate height separation away from the microstrip. Furthermore, to confine electromagnetic fields within the two via fences via-to-via spacing  $L$  has to be less than or equal to  $2.5H$ . The extracted insertion loss for a single transition is less than 1.25 dB over 75% of the transmission band and return loss is more than 10 dB over the entire bandwidth. The performance of the transition can be improved by using thinner substrate as less electric field will be confined in the dielectric under the probe. The integrated probe provides direct coupling to WR-10 waveguide without ribbon bonding or external transitions.

## REFERENCES

1. Reljic, B. M., "Low loss MIC/MMIC compatible microstrip to waveguide transition without a balun," *Microw. Optical Tech. Lett.*, Vol. 50, No. 1, 107–111, Jan. 2008.

2. Bai, R., Y.-L. Dong, and J. Xu, "Broadband waveguide-to-microstrip antipodal finline transition without additional resonance preventer," *IEEE Int. Symp. Microw. Antenna, Propagation, and EMC Tech. for Wireless Comm.*, 385–388, 2007.
3. Kaneda, N., Y. X. Qian, and T. Itoh, "A broad-band microstrip-to-waveguide transition using quasi-Yagi antenna," *IEEE Trans. Microw. Theory Tech.*, Vol. 47, No. 12, 2562–2567, Dec. 1999.
4. Grabherr, W., B. Huder, and W. Menzel, "Microstrip to waveguide transition compatible with mm-wave integrated circuits," *IEEE Trans. Microw. Theory Tech.*, Vol. 42, No. 9, 1842–1843, Sep. 1994.
5. Leong, Y.-C. and S. Weinreb, "Full band waveguide-to-microstrip probe transitions," *IEEE MTT-S Symp. Dig.*, Vol. 4, 1435–1438, 1999.
6. Nguyen, B. D., C. Migliaccio, C. Pichot, and N. Rolland, "Design of microstrip to waveguide transition in the W band suitable antenna or integrated circuits connections," *Microw. Optical Tech. Lett.*, Vol. 47, No. 6, 518–520, Dec. 2005.
7. Weinreb, S., T. Gaier, R. Lai, M. Barsky, Y. C. Leong, and L. Samoska, "High-gain 150–215 GHz MMIC amplifier with integral waveguide transitions," *IEEE Microw. Guided Wave Lett.*, Vol. 9, No. 7, 282–284, Jul. 1999.
8. Ponchak, G. E., D. Chun, J.-G. Yook, and L. P. B. Katehi, "The use of metal filled via holes for improving isolation in LTCC RF and wireless multichip packages," *IEEE Trans. Microw. Theory Tech.*, Vol. 23, No. 1, 88–99, Feb. 2009.